Improved Evaluation of Interface Friction on Steel Pipe Pile in Sand

Feng Yu[1] and Jun Yang, M.ASCE[2]

Abstract: Open-ended steel pipe piles are now widely used as the foundations for offshore structures. The pile-soil interface behavior is of particular interest in sands where shaft friction plays an important role in resisting the applied load. The rational design of the shaft capacity depends on a good understanding of the mechanisms of interface friction during pile installation and static loading. There are two new methods on the basis of the cone penetration test results that take into account the effect of friction fatigue arising from pile installation. An improvement is made in this study to account for the influence of plugging degree, which is a key issue for open-ended piles. The significance of the modified design framework lies in that it allows for the role of plugging in a more rational way by using the soil-squeezing ratio that is closely related to the radial effective stress and, consequently, the shaft capacity. The performance of the improved method is assessed against the existing methods in terms of evaluating the shaft resistance of two full-scale offshore bridge piles. **DOI: 10.1061/(ASCE)CF.1943-5509.0000256.** *© 2012 American Society of Civil Engineers.*

CE Database subject headings: Pipe piles; Steel piles; Sand (soil type); Cone penetration tests; Shafts; Friction; Fatigue; Case studies.

Author keywords: Steel pipe piles; Sand; Cone penetration test; Shaft capacity; Friction fatigue; Case history.

Introduction

Construction of many important offshore facilities such as cross-sea bridges widely involves the use of open-ended steel pipe piles as deep foundations because of their favorable drivability. Estimation of the capacity of pipe piles is one of the fundamental issues in pile design and involves great uncertainty. While a number of analytical and numerical methods have been developed for this purpose, empirical correlations on the basis of in situ geotechnical tests appear to be widely relied on (Randolph 2003). Among the in situ tests, the cone penetration test (CPT) has been preferably used in the development of the relationship between the cone resistance and pile capacity. This is because the CPT resembles pile penetration and loading, and that the CPT is routinely used in ground investigation. This test is capable of measuring the cone sleeve friction (f_s) and cone-tip resistance (q_c) at any depth. As the measurement of q_c is more reliable than that of f_s, the q_c profile is widely used to correlate with both the shaft and the base resistances of piles (Schneider et al. 2008). More recently, several CPT-based methods for estimation of the capacity of pipe piles with improved reliability and rationality have been developed (e.g., Jardine et al. 2005; Lehane et al. 2005).

Deep foundations in the marine environment usually make use of sandy deposits as the main pile-supporting strata. The axial shaft capacity of an open-ended steel pipe pile in sandy soil can be influenced by a number of factors arising from driving or jacking installation, particularly by the soil-plugging behavior and the degradation of shaft friction. These influencing factors need to be carefully taken into consideration in CPT-based design methods. This paper presents a framework to correlate the CPT cone-tip resistance with the local shaft capacity of open-ended steel pipe pile in sand. An improvement is made to incorporate a so-called soil-squeezing ratio into the correlation, by examining the mechanism of interface shear. The accuracy of the proposed design framework is assessed by using full-scale field-test data.

Interface Shear Behavior

Current understanding of the local shaft capacity of pile (τ_s) in sand is based on the Coulomb failure criterion as given in Eq. (1), where τ_s equals the local radial effective stress acting on the pile wall at failure, σ'_r, multiplied by the interface friction coefficient, tan δ

$$\tau_s = \sigma'_r \tan\delta = (\sigma'_{rc} + \Delta\sigma'_r)\tan\delta \quad (1)$$

The variables σ'_{rc} and $\Delta\sigma'_r$ in Eq. (1) represent, respectively, the radial effective stress at the stationary status before static loading and the increase attributable to static loading; and δ = pile-soil interface friction angle at failure. Despite the simplicity in format, great uncertainty arises from the absence of adequate knowledge on assessing the σ'_r, $\Delta\sigma'_r$ and δ for displacement piles in sand.

The radial effective stress is apparently the key parameter to properly estimate the local shaft capacity. A close-up view of the sand particles surrounding a penetrating pile may shed light on the behavior of deformation and associated stress near the shaft. White and Bolton (2002) found that high particle breakage occurred in a narrow shear zone surrounding the pile shaft. The densification and contraction of sand during penetration will impose a negative effect on the variation in the radial effective stress, hence reduce the local shaft friction. Figs. 1(a) and 1(b) offer a schematic illustration of the development of shear zone around the shaft during installation and static loading of an open-ended pipe pile in sand. The normal stiffness of the in situ soil surrounding an axially loaded pile is defined

[1]Associate Professor, School of Civil Engineering and Architecture, Zhejiang Sci-Tech Univ., Hangzhou 310018, China (corresponding author). E-mail: pokfulam@163.com

[2]Associate Professor, Dept. of Civil Engineering, The Univ. of Hong Kong, Pokfulam Road, Hong Kong, China. E-mail: junyang@hku.hk

Note. This manuscript was submitted on August 20, 2010; approved on June 14, 2011; published online on June 16, 2011. Discussion period open until September 1, 2012; separate discussions must be submitted for individual papers. This paper is part of the ***Journal of Performance of Constructed Facilities***, Vol. 26, No. 2, April 1, 2012. ©ASCE, ISSN 0887-3828/2012/2-170–179/$25.00.

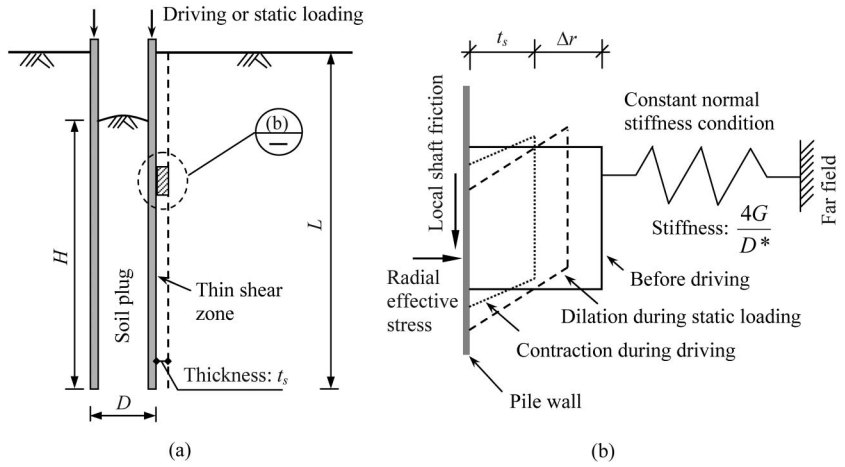

Fig. 1. Behavior of the shear zone during installation and static loading: (a) schematic diagram of the shear zone; (b) variation in the shear zone

as the ratio of the variations in the radial stress to the radial displacement. The condition of constant normal stiffness (CNS) can well simulate the real soil field (Fakharian and Evgin 1997). As pile driving releases the lateral confinement, the densified shear zone tends to dilate during the subsequent stage of working condition or loading test. This inversely gives rise to an increase in the radial effective stress. The shear zone under CNS and cyclic loading conditions is found to have an accumulation of residual shear displacement, which is possibly the trigger of reducing the radial effective stress. An increase in the cumulative shear displacement leads to an increase in the thickness of the shear zone (t_s) that ranges between 3.5 and 5.5 mm for silica sand (DeJong et al. 2003). The degree of reduction can be greater if greater CNS and more loading cycles are applied.

Field tests on displacement piles in sand have shown that the reduction in the radial effective stress at a given horizon will be greater as the pile penetrates deeper (Lehane et al. 1993). Such degradation of shaft resistance has been recognized for decades and generally referred to as "friction fatigue" (White and Lehane 2004). The friction fatigue is likely to be closely related to the persistent contraction of shear zone during pile penetration. The major CPT-based design methods (e.g., Randolph et al. 1994; Jardine et al. 2005; Lehane et al. 2005) have introduced empirical reduction factors to characterize the depth-related degradation of shaft resistance. However, the rate of degradation has been noticed to be strongly affected by the method of pile installation. Paik and Salgado (2004) noted from testing model pipe piles that the shaft capacity of a jacked pile was greater than that of an identical driven pile. The observation reveals that current design methods are not able to capture some essential mechanisms responsible for friction fatigue.

It is worthy to note the centrifugal model pile tests conducted by White and Lehane (2004) who observed the stationary radial effective stresses of piles installed by monotonic, jacked, and pseudodynamic methods. A monotonic pile may be deemed as a one-stroke jacked pile that does not involve the reversal of shear displacement and the accumulation of residual shear displacement. The pseudodynamic method involves two-way cycles of greater downward and smaller upward displacements to simulate the installation procedure of driven piles in the absence of dynamic effect. The value of σ'_{rc} is found to be closely dependent on the number of loading cycles during installation (Fig. 2). The test data inferred from different installation methods tend to follow a unified trend line expressed by

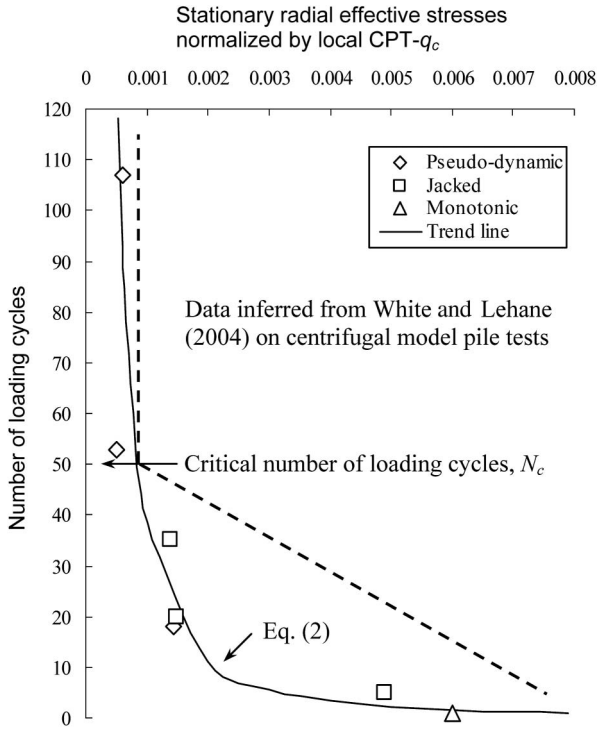

Fig. 2. Dependence of the normalized stationary radial effective stress on loading cycles (White and Lehane 2004)

$$\sigma'_{rc} = 0.0079N^{-0.5664}q_c \tag{2}$$

where q_c and N = local CPT cone-tip resistance and the number of loading cycles experienced by the soil at a given horizon during installation, respectively. In practical situation, N is similar to the number of press-in strokes for jacked piles or blow counts for driven piles received at any depth. This indicated that the number of jacking strokes or blow counts during pile construction is very likely one of the indices to reflect the decay in radial effective stress and subsequently shaft friction. As described previously, observations on the shear zone reveal that increase in the number of loading cycles gives rise to the accumulation of shear displacement, which is a more essential parameter to represent friction fatigue than the cycle number. This viewpoint is supported by the boundary element analysis of Poulos (1989) who discussed the

importance of cumulative shear displacement to determine the shaft friction under one-way cyclic loading similarly to pile installation.

The accumulated residual shear displacement in the shear zone or more apparently the experienced number of loading cycles capable of mobilizing peak shear strength is proved by the previous analyses to be the essential index to represent the degradation of shaft friction. These two indices, however, are inconvenient for reliable measuring or estimate. Although Eq. (2) is likely to reveal the underlying mechanism of friction fatigue, it may not be applied to practical design. The magnitude of σ'_{rc} predicted by Eq. (2) is normally one order lower than the field measurements of offshore test piles such as the Fugro pile (White and Lehane 2004) and the Euripides pile (Jardine et al. 2005). What can be clearly captured in Fig. 2 is that the normalized radial effective stress drops sharply during the initial tens of cycles then decreases more slowly when N is in excess of $N_c(\approx 50)$. This variation in σ'_{rc}/q_c is enveloped and overestimated by a folded line. Direct shear tests under CNS condition also confirm that the rate of reduction in shear stress is higher during the first few cycles (Fakharian and Evgin 1997).

The statistical charts in Fig. 3 show the mean blow counts or loading cycles required for 1 m of pile penetration. A total number of 5,192 steel pipe piles used for the cross-sea bridge of Hangzhou Bay, China are involved in the analysis (Wang 2008). The piles are driven into multilayered soils primarily consisting of clay and sand. The friction angles of the soils range from 15° to 20° for clay and from 33° to 36°for sand. Most piles receive averagely $18 \sim 40$ blows per meter for the entire pile length. The actual blow counts increase rapidly during the terminative penetration stage so as to satisfy the final-set requirement of normally less than 10 mm in one blow. This implies that the soil adjacent to an offshore steel pipe pile may experience hundreds or thousands of loading cycles during installation. Referring to Fig. 2, complete decay in shaft friction will take place for an offshore pile in practice, except the soil near the pile base.

From Fig. 4, the accumulated shear displacement and the number of loading cycles are inconvenient for real use, although both are fundamental indices. Despite the availability of blow–count record for pile driving, it is not easy to match the blow-count with the penetration record especially at small penetration rate (e.g., at final set). Difficulty arises in confirming the experienced number of loading cycles for deep soil adjacent to pile base. Instead, the apparent depth index is much suitable provided that due consideration is paid on reducing the uncertainty in prediction. The effect of pile-installation method may be taken into account in an alternative way.

Existing Design Methods

Several design methods have been established on extensive load-test database that include the friction fatigue in terms of depth index. Two of them, namely the Imperial College Pile (ICP) (Jardine et al. 2005) and the University of Western Australia (UWA) (Lehane et al. 2005) methods, respectively, appear to be widely recognized and are briefly reviewed in this paper.

The ICP method uses the following expression to evaluate the local shaft capacity:

$$\tau_s = 0.029(\sigma'_{v0}/p_a)^{0.13}[\max\ (h/R_e, 8)]^{-0.38} q_c \tan \delta_{cv} + \Delta\sigma'_r \tan \delta_{cv} \quad (3)$$

where σ'_{v0} local effective overburden pressure before pile installation; p_a = atmospheric pressure equal to 100 kPa; h = distance of the observed level from the pile tip; R_e = equivalent pile radius equal to $0.5(D^2 - d^2)^{0.5}$ in which D and d are, respectively, the outer and inner diameters of the pile and δ_{cv} = constant volume

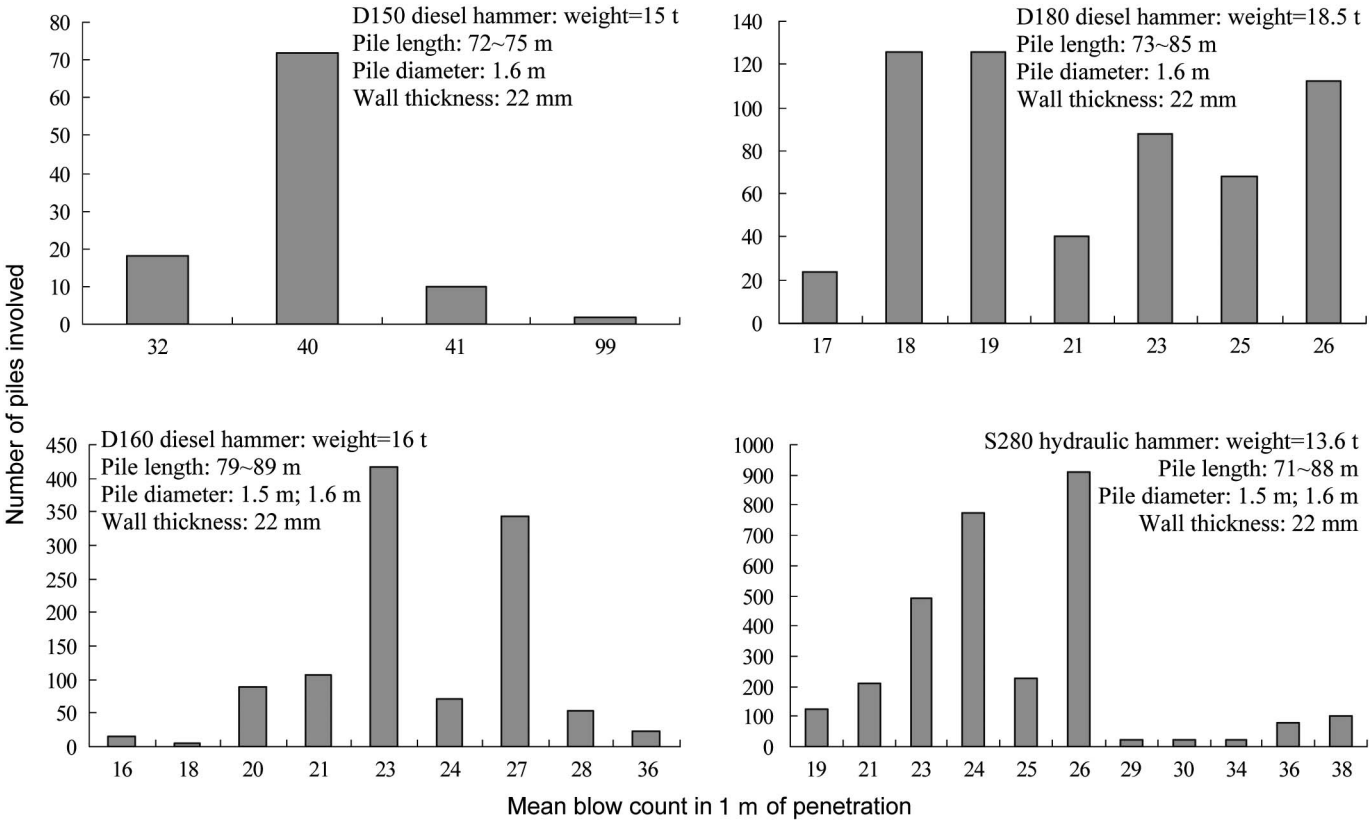

Fig. 3. Statistics of blow counts of steel pipe piles used in the cross-sea bridge of Hangzhou Bay

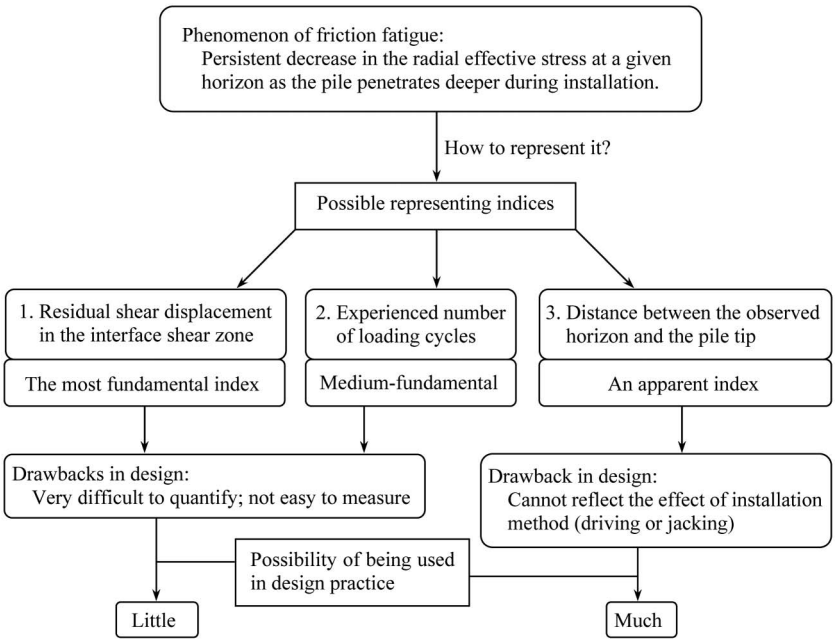

Fig. 4. Decision in choosing an appropriate index to represent friction fatigue in pile design

friction angle at the pile-soil interface. The term "h/R_e" represents the stress relief in radial direction at a given horizon of h over the pile tip, e.g., the degradation of local shaft friction. A lower bound of "$h/R_e = 8$" is applied so that the calculated stress remains constant over the bottom $8R_e$ pile length. The equivalent radius of pipe pile is introduced to account for the degradation of σ'_r led by the constant volume penetration of an equivalent solid pile.

The magnitude of $\Delta\sigma'_r$ from loading to failure is associated with the behavior of the thin interface shear zone responsible for the radial displacement. The importance of $\Delta\sigma'_r$ increases with decreasing pile diameter. The magnitude of $\Delta\sigma'_r$ is normally positive because of the dilation of sand, and the ICP method adopts a cavity expansion solution to evaluate this increase by

$$\Delta\sigma'_r = 4G\Delta r/D \tag{4}$$

where G = shear modulus of the surrounding soil that can be empirically determined from CPT point resistance; and Δr= radial displacement developed within the pile-soil interface shear zone during loading.

The UWA method is developed on the basis of the ICP method. They are similar in many aspects, but the UWA method is primarily formed for offshore driven piles in sand. For piles in compression, this method suggests that the shaft resistance is estimated as

$$\tau_s = 0.03[1 - (d/D)^2\text{IFR}]^{0.3}[\max\ (h/D,\ 2)]^{-0.5}q_c \tan\delta_{cv} + \Delta\sigma'_r \tan\delta_{cv} \tag{5}$$

where IFR = incremental filling ratio of soil plug averaged over the last $3D$ of pile penetration; $\Delta\sigma'_r$ is calculated in the same manner as Eq. (4). For piles subjected to tension loading, Eq. (5) is multiplied by 0.75.

Fig. 5 presents a calculation example for open-ended pile using the ICP and UWA methods. Compared with Fig. 2 in which the index of the number of loading cycles is involved, the calculated distributions in Fig. 5 show consistency in the rate of reduction in radial effective stress with the depth index. The shallower soil receives much more blow counts than the deeper soil to satisfy the final-set requirement for a driven pile. This leads to the number of

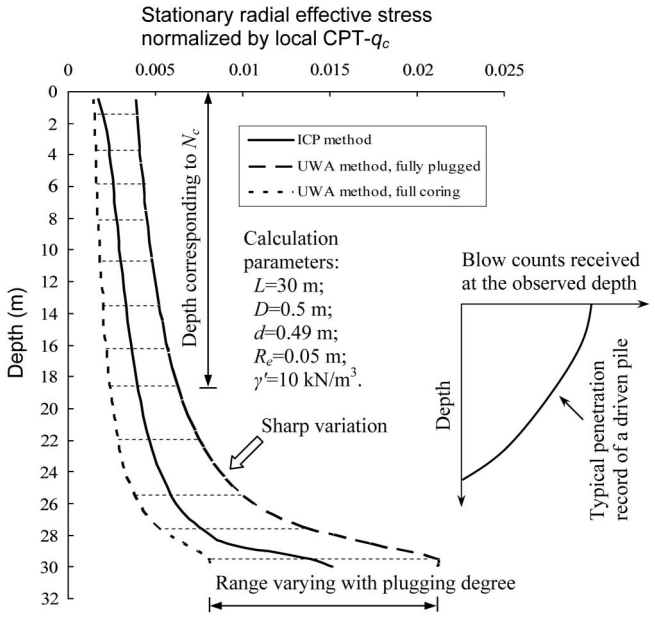

Fig. 5. An example of the σ'_{rc}/q_c for open-ended pile using the ICP and UWA methods

loading cycles experienced at shallow depth normally in excess of N_c and the occurrence of full decay in the radial effective stress. For deeper depth where fewer loading cycles have been experienced, with respect to Fig. 2, the variation in the radial effective stress is more sensitive with the cycle number and, consequently, the depth. This demonstrates the applicability of using the apparent depth index to represent friction fatigue. Overall, similar results are yielded by the two methods, and the curve of the ICP method falls into the range of the UWA method, which is able to consider the effect of plugging degree. Database studies show that the UWA method, achieves the best agreement with field data among the CPT-based methods adopted by the American Petroleum Institute practice (Schneider et al. 2008).

Modified Design Approach

Plugging Behavior and Soil-Squeezing Ratio

Soil plug can be formed in an open-ended pipe pile that causes less radial soil displacement than that of a closed-ended one. The plugging behavior has been extensively studied primarily to achieve better understanding of the end-bearing performance. Its effect on the shaft friction, however, has not been investigated systemically. Fig. 6 illustrates four piles with the same length and outer diameter driven into the ground. Installation of the closed-ended pile (or solid pile) leads to full displacement of soil, allowing a cylindrical expansion equal to the enveloped volume of the pile body. For an open-ended pile of no soil coming into the pipe, the induced soil displacement is very similar to that of the closed-ended pile. The radial soil displacement and, consequently, the radial effective stress acting on the shaft are closely related to the elevation of soil plug during installation.

It is noted that pile design methods normally recommend different modifying factors for the unit shaft capacity with respect to the difference in pile end condition; lower values are applied to open-ended piles and higher values are equally devoted to closed-ended and solid piles [Randolph 2003; Geotechnical Engineering Office (GEO) 2006]. Yu and Zhang (2011) analyzed the discrepancy in shaft capacities of open-ended and closed-ended pipe piles, and pointed out that the reduction factor attributable different radial soil displacements ranged from 0.4 to 0.6 for steel pipe piles. The configuration of open-ended steel pipe pile (i.e., relatively small wall thickness and large inner diameter) is responsible for such remarkable reduction in shaft capacity compared with the closed-ended type. Some field tests also demonstrate the significant influence of the amount of radial soil displacement on the mobilized shaft friction (Paik et al. 2003). It is therefore important to take into account the effect of soil plugging and the associated radial soil displacement. The previously discussed literatures have involved a simple consideration on the end condition of pipe pile. However, the influence of different elevations of soil plug on the reduction degree (e.g., the first three piles in Fig. 6) is yet an issue to be explored.

A practical solution is to correlate the volume of displaced soil caused by pile installation to the degree of soil plugging. The UWA method introduces the index, IFR, to allow for plugging degree. With the Coulomb failure criterion, Eq. (5) can be rewritten in the following form:

$$\sigma'_{rc} = 0.03[1 - (d/D)^2\text{IFR}]^{0.3}[\max\ (h/D,\ 2)]^{-0.5} q_c \qquad (6)$$

The term "$1 - (d/D)^2$ IFR" can be regarded as an effective area ratio ($A_{r,\text{eff}}$) that reflects the influence of soil plugging. $A_{r,\text{eff}}$ equals $1 - (d/D)^2$ and 1, respectively, for the modes of full coring and fully plugged. The parameter IFR is not easy to determine in practical application because it requires continuous measurements of the plug length and penetration depth during the final driving stage. To overcome this difficulty and, moreover, to allow for the plugging effect in a more rational way, an alternative approach is proposed in this paper.

A concept known as "soil-squeezing ratio" (ρ) is introduced as

$$\rho = 1 - \text{PLR}\ (d/D)^2 > 0 \qquad (7)$$

where PLR = plug length ratio at the final penetration. Referring to Fig. 6, PLR $= H/L$. Obviously, the soil-squeezing ratio equals the volume of soil squeezed during pile penetration divided by the volume of an identical solid or closed-ended pile. Regardless of the densification of soil, the volume of squeezed soil can be determined as a sum of the vacancy over the upper portion in the pipe plus the annulus volume of the pipe (Fig. 6). The rationality of replacing the index of IFR by PLR lies in that direct relationships can be established between the length of plug, the volume of squeezed soil, and the reduction in radial effective stress and shaft friction. Referring to the three open-ended piles in Fig. 6, the value of IFR at the final installation is likely to be any quantity between 0 to 1, depending on the end-bearing soil and driving record. Therefore, the influence of radial soil displacement at different elevations of soil plug cannot be explicitly reflected by the IFR.

Eq. (7) has a similar form with $A_{r,\text{eff}}$, but it uses the more reasonable and easily measured index, PLR, to represent the effect of plugging degree. In the case that the soil plug is elevated to a level higher than the ground surface or seabed, i.e., PLR $(d/D)^2 > 1$ is satisfied, an additional requirement of $\rho > 0$ shall be applied in Eq. (7).

Radial Effective Stress

Assuming the depth of an observed soil horizon to the ground surface or seabed level is equal to ξL, where L is the pile length and

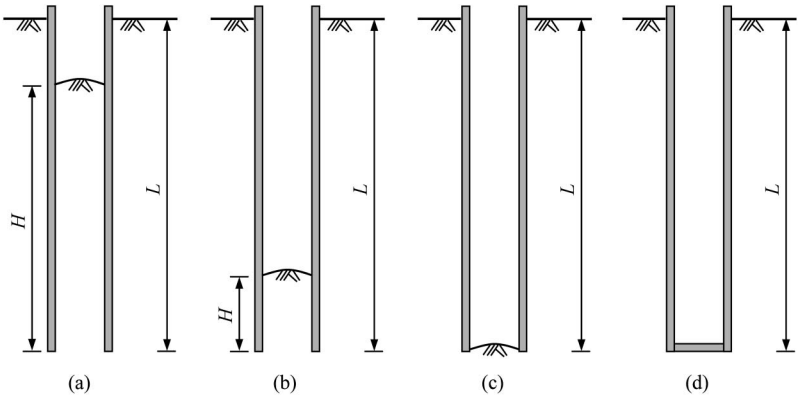

Fig. 6. Schematic showing the phenomena of soil plugging and soil squeezing: (a) open-ended pile, higher elevation of plug, unknown plugging mode; (b) open-ended pile, lower elevation of plug, unknown plugging mode; (c) open-ended pile, no elevation of plug, plugged mode; (d) closed-ended pile, no elevation of plug, full-displacement mode

$0 \le \xi \le 1$, the stationary radial effective stress involving the effect of soil-squeezing ratio can be computed by using Eqs. (6) and (7)

$$\sigma'_{rc} = 0.03\rho^{0.3}(L/D)^{-0.5}(1-\xi)^{-0.5}q_c \le 0.021\rho^{0.3}q_c \quad (8)$$

An additional term, "$0.021\rho^{0.3}q_c$," is imposed to avoid the unreasonable increase caused by the regression trend in a power function. Eq. (8) facilitates an easy estimate of σ'_{rc}/q_c by the ratio of pile length to diameter and the PLR.

The increase in radial effective stress attributable to static loading can be evaluated by the cavity expansion solution, as shown in Eq. (4) where the term "$4G/D$" = CNS simulating the in situ lateral constraint [Fig. 1(b)]. The penetration problem in cavity expansion analysis usually treats piles as closed-ended or solid type. The initial cavity radius resembles the volume change of soil mass attributable to penetration. In this concern, a modified diameter, D^*, instead of D is more appropriate in using Eq. (4) for open-ended pipe piles. By regarding D^* as the diameter of an equivalent closed-ended or solid pile that causes the same volume change as an open-ended pile with diameter of D, D^* can be assessed by $D^* = (D^2 - \text{PLR } d^2)^{0.5}$. Thus, Eq. (4) is modified as

$$\Delta\sigma'_r = 4G\Delta r/(D^2 - \text{PLR } d^2)^{0.5} \quad (9)$$

which indicates that a full coring pile will have smaller modified diameter and, consequently, greater increase in radial effective stress during static loading.

The shear modulus of soil can be evaluated according to the local cone-tip resistance. This study follows the UWA method to use (Lehane et al. 2005).

$$G = 185\frac{(q_c/p_a)^{-0.7}}{(\sigma'_{v0}/p_a)^{-0.35}}q_c \quad (10)$$

The ICP method employs a similar correlation (Jardine et al. 2005) to compute the shear modulus that is close to the output of Eq. (10). The radial displacement of the shear zone, Δr, is related to the thickness and dilation of the shear zone and normally equals to 0.02 mm for slightly rusted steel surface in sand (Jardine et al. 2005).

Interface Friction Angle

Local shear failure will take place in the surrounding soil rather than along the pile-soil interface if the roughness at the pile surface is adequately large (Uesugi and Kishida 1986), such as the deeply rusted steel piles over long work duration. However, it is difficult to judge where the shear failure will occur as early as during the design phase. Conservative approach may be adopted to assume a failure along the pile-soil interface.

The magnitude of δ lies in a typical range of 0.6 to 0.7 times the peak effective friction angle of sand (Randolph et al. 1994). A simple shear test is routinely used to find the values of δ for a variety of sand and steel surfaces. Some important factors having great influence on the pile-soil interface friction angle include the type and particle size distribution of sand, and the surface roughness. Cyclic loading also imposes effect on reducing the magnitude of interface friction angle that eventually converges at the residual shear stress ratio of sand (Uesugi and Kishida 1986; Uesugi et al. 1989). This may be an indicator of the validity on substituting δ by the constant volume interface friction angle, δ_{cv}, which has been adopted by the ICP and UWA methods. The value of δ_{cv} decreases with increasing mean particle size (d_{50}) and ranges typically between 28° to 29° for siliceous sand (Jardine et al. 2005). In the UWA method, an upper limit of $\delta_{cv} = 29°$ is applied to fine-grained sand (Lehane et al. 2005).

Further Consideration

The overall shaft capacity of an open-ended pile (Q_s) can be assessed by

$$Q_s = \pi DL\tan\delta\int_0^1(\sigma'_{rc} + \Delta\sigma'_r)d\xi \quad (11)$$

where σ'_{rc} and $\Delta\sigma'_r$ are evaluated by Eqs. (8) and (9), respectively. The value of δ is equal to δ_{cv} by assuming a failure along the pile-soil interface. The shear modulus of soil may be derived from Eq. (10). The integration in Eq. (11) can be solved by dividing the pile shaft into adequately short segments. Separated sections should be applied to the situation of soil layering or extreme variation in CPT $-$ q_c profiles. The proposed approach also needs information on the PLR that is convenient to obtain. In case of unknown PLR, its magnitude needs to be estimated in advance of design. It is very likely that the PLR varies inversely with the ratio of pile length to inner diameter (Yu and Zhang 2011).

For jacked piles, as the push-in distance of one jacking stroke generally ranges within $1 \sim 2$ m, the total strokes required for jacking a pile are potentially less than the critical number of loading cycles (N_c). For long driven piles frequently used as offshore infrastructures, the total blow count in excess of 1,000 is common. Furthermore, the final-set requirement leads to the occurrence of much blow count consumed within the final small penetration. In this sense, jack piling is innovative for displacement pile installation compared with the traditional percussive methods. This study also supports the fact that jacked piles essentially have greater shaft capacities than identical driven piles by introducing the parameter of PLR, as jacked pipe piles normally have smaller values of PLR and subsequently larger soil-squeezing ratios than driven pipe piles (Paik and Salgado 2004; Yu and Zhang 2011).

Case Studies of Offshore Piles

To examine the applicability of the ICP, UWA, and the modified methods for the design of offshore foundations, a case history containing two large-diameter open-ended steel pipe piles in granular soils is presented in this paper (Kikuchi et al. 2007). The two test piles, namely TP4 and TP5, were located in Tokyo Port Bay where the Tokyo Coastal Highway Bridge was planned to construct. Open-ended steel pipe piles were designed to serve as the pier foundations of the bridge. For lack of full understanding on the prospective performance of such piles, static load tests were performed on the two trial piles to investigate their serviceability that could be applied in the formal use.

The outer diameter and wall thickness of the test piles were 1.5 m and 28 mm, respectively. The piles were installed by percussive method with S280 hydraulic hammer to reach embedded lengths of 73.5 m for TP4 and 86 m for TP5. The piles were driven first through a thick layer of alluvial soil in soft and cohesive state with thickness of 33 m, and then into layered soils with alternating clay and sand with thickness of 25 m, and finally down to stiffer granular soils. The bearing strata for TP4 and TP5 were sandy gravel and sand layers, respectively. The portions of the piles adjacent to the pile bases, i.e., 64.1-73.5 m for TP4 and 77-86 m for TP5, were embedded in sandy soils. The blow counts of standard penetration test within these two portions normally ranged from 40 to 50. Relevant CPT $-$ q_c trace is given in Fig. 7(a).

The test piles were instrumented with strain gauges along the shafts that facilitated the measurements of pile-load transfer

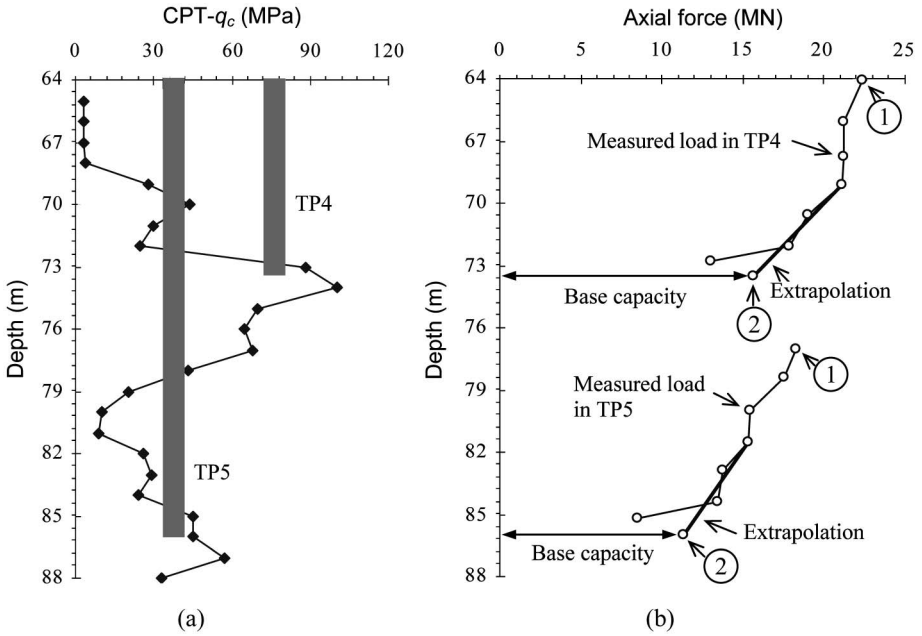

Fig. 7. Information on the test site and piles used in the case studies (Kikuchi et al. 2007; Xu et al. 2008): (a) CPT $-$ q_c profile; (b) measured axial force distributions along TP4 and TP5

subjected to axial loading. The static load test followed a sequence of multistage repeated loading in which the applied load at a stage was maintained until the pile-head settlement was not larger than the target value. The load distribution shown in Fig. 7(b) corresponds to a pile-base displacement of 10% diameter, implying that the shaft friction has been fully mobilized. As the strain gauges recorded a combination of resistances provided by the plug and external soil, Kikuchi et al. (2007) introduced an approximation of linear extrapolation to exclude the internal friction from the shaft component [Fig. 7(b)]. The extrapolation was based on the assumption that an abrupt and sharp decrease in the axial force was the result of plug resistance being mobilized. This method has sound background because the soil near the pile base does not show sudden increase in strength, and the internal friction of soil plug is generally concentrated over 1D above the pile-base (Randolph 2003). In addition, the derived base capacity was verified against the empirical correlation proposed by de Nicola and Randolph (1997), and a satisfying agreement was achieved. Thus, the shaft capacities gained within the observed ranges can be well determined as the differences between the points 1 and 2 in Fig. 7(b).

The test piles are very long in length; hence, referring to Fig. 3 for S280 hydraulic hammer, the experienced number of driving cycles will be adequate for full decay in friction to take place (see Fig. 2). Furthermore, the thin-walled configuration of steel pipe pile possibly gives rise to smaller radial soil displacement during installation. These two features can impose significant effect on the shaft capacity. The well-recognized effective stress method introduces the coefficient of $\beta(=\tau_s/\sigma'_{v0})$ for shaft capacity design. By taking the average of the shaft capacity and the overburden pressure over the concerned depth, the mean β values of the two piles can be back-calculated to be 0.183 for TP4 and 0.169 for TP5. The magnitude is far below some back-analysis results on shorter and thicker-walled prestressed concrete pipe piles driven in decomposed granitic soil whose property is close to silty sand (GEO 2006). The considerable deviation in the β values can be attributed to the effects of friction fatigue and soil plugging. Implications may be drawn that for the design of long steel pipe piles, the influence of relatively small soil-squeezing ratio and full degradation of friction should be addressed in assessing the shaft capacity.

The two piles were driven in the full coring mode. The plug levels were observed to exceed the seabed. Also, note in the UWA method that the IFR can be approximately judged as (Lehane et al. 2005)

$$\text{IFR} = \min\ [1,\ (d/1.5)^{0.2}] \tag{12}$$

where d is in meter. The calculated IFR is close to unit. Therefore, it is reasonable to adopt PLR $= 1$ and IFR $= 1$ in the assessment. Moreover, a mean effective unit weight of soil equal to 12 kN/m^3 is used. A typical value of $\delta_{cv} = 29°$ (Jardine et al. 2005) may be adopted in case that shear test results are unavailable. By employing the CPT $-$ q_c data in Fig. 7(a), one is able to compute the values of σ'_{rc}, $\Delta\sigma'_r$ and τ_s by sequence.

The results are given in Figs. 8–10 and Table 1, where Q_m and Q_c = measured and calculated shaft capacities, respectively. With respect to the stationary radial effective stress (Fig. 8), the predictions by the ICP method are greater than the other two. Both the IFR and PLR are equal to 1; the values of σ'_{rc} calculated by the UWA method and this study are very close. As for the increase in radial effective stress because of static loading (Fig. 9), the predictions by this study are much greater than those by the ICP and UWA methods. This is because a modified diameter is involved to evaluate the $\Delta\sigma'_r$ for open-ended piles in this study. The distributions of the local unit shaft capacities generally trace the CPT $-$ q_c trend. The predictions of this study lie between the ones derived from the ICP and UWA methods (Fig. 10). Regarding the overall shaft capacities within the observed depths, this study provides the best agreement with the field measurements that are overestimated by 30% more in the ICP method and underestimated by 15% more in the UWA method (Table 1).

As the three methods are developed on a similar background, the discrepancies in prediction accuracy may be attributed largely to the different considerations of soil-squeezing ratio and friction decay rate. The overestimation of the ICP method is caused by the use of smaller rate of friction fatigue and the greater prediction of stationary radial effective stress. This study follows the friction

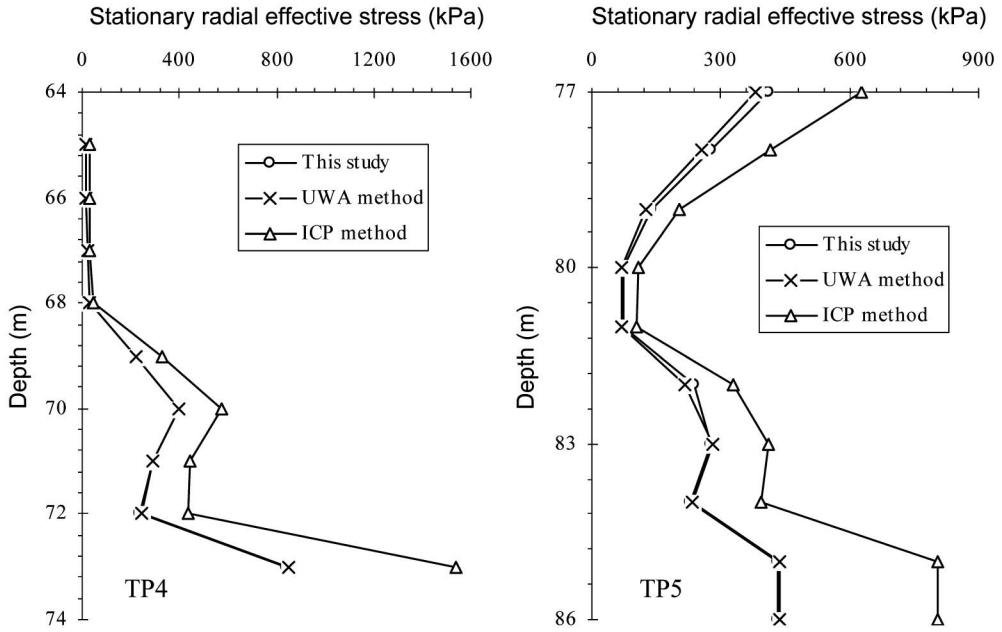

Fig. 8. Predicted stationary radial effective stresses before static loading for TP4 and TP5

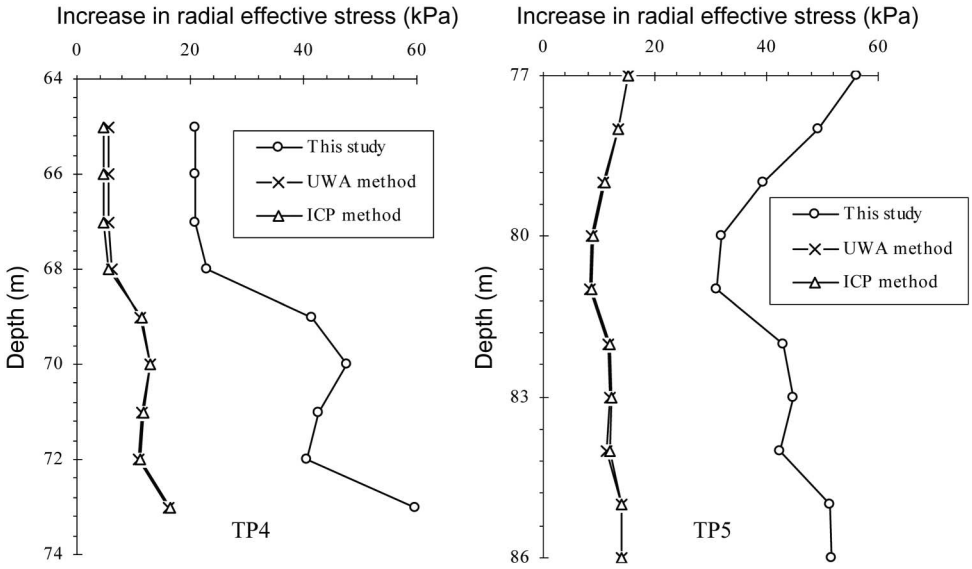

Fig. 9. Predicted increases in radial effective stress attributable to static loading for TP4 and TP5

decay rate adopted in the UWA method, but differs in the consideration of plugging degree. A proper evaluation of the stress increase attributable to static loading in this study may simulate more closely the axial loading behavior of open-ended piles. The comparison shows that the modified approach has advantage over the other two CPT-based methods because a rational consideration of the soil-squeezing degree has been allowed for.

Discussions

Entire-Process Variation in Interface Friction

Fig. 11 illustrates the time-related change of radial effective stress acting on the pile shaft at different stages. Friction fatigue is the main trigger of reducing the initial radial effective stress during the pile-driving stage. The reduction rate is closely dependent on the number of loading cycles. The "fresh" pile is then subjected to static loading that leads to an increase in radial effective stress. The magnitude of $\Delta\sigma'_r$ relies on the dilation of shear zone and the rotation of principal stress, which impose positive and negative effects, respectively. The shaft capacity gained immediately after static loading may be called "static and fresh" capacity (Jardine et al. 2005), which is the major concern of this study.

An offshore pile is likely to experience a number of wave- and wind-induced loading cycles, which further reduce the radial effective stress, The post-installation degradation of shaft friction has been studied by Poulos (1989), and Chin and Poulos (1996) who found that the interface shear displacement had significant influence on the decay in radial effective stress. Their findings are consistent with the microscopic observations on the factors affecting the friction fatigue (e.g., DeJong et al. 2003). Therefore, the

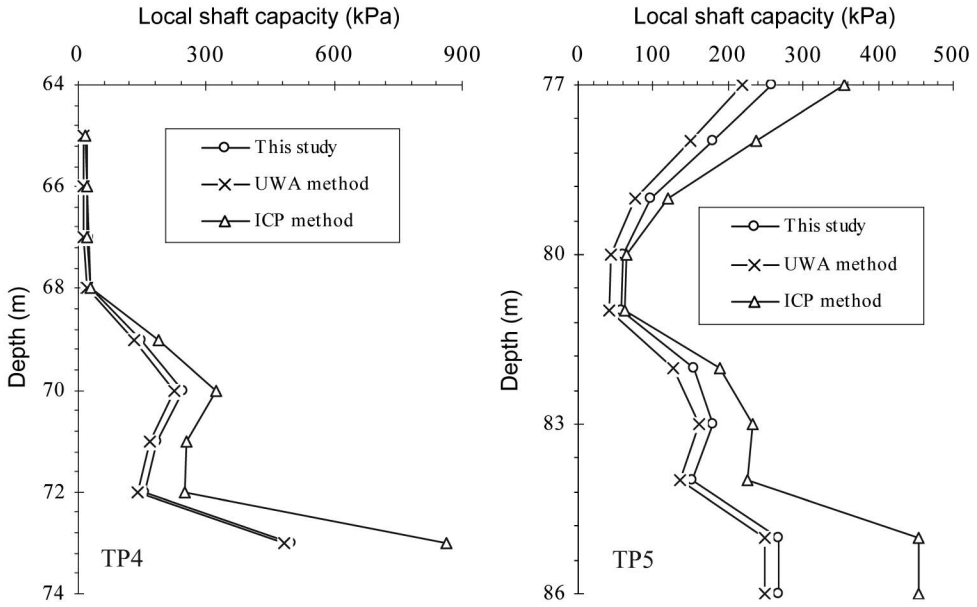

Fig. 10. Predicted local shaft capacities for TP4 and TP5

Table 1. Measured and Calculated Shaft Capacities for TP4 and TP5

Pile number	Range of depth concerned (m)	$Q_m(kN)$	ICP method		UWA method		This study	
			$Q_c(kN)$	Q_c/Q_m	$Q_c(kN)$	Q_c/Q_m	$Q_c(kN)$	Q_c/Q_m
TP4	64.1–73.5	6,700	9,279	1.38	5,691	0.85	6,276	0.94
TP5	77–86	7,000	9,370	1.34	5,738	0.82	6,641	0.95

Note: Q_m, measured shaft capacity; Q_c, calculated shaft capacity.

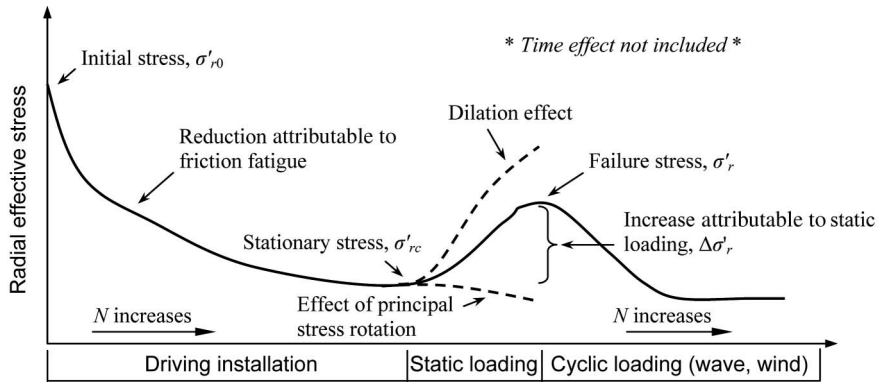

Fig. 11. Schematic diagram of the variation in radial effective stress

reduction in shaft friction both at the installation and working stages is possibly correlated to the same index, number of loading cycles. Despite the similarity in mechanism, the post-installation degradation of shaft friction may be less affected by the cycle number as the majority of the wave- and wind-induced loading cycles fail to mobilize sufficient local shear displacement.

What has not been illustrated in Fig. 11 is the long-term increase in shaft capacity that could be very large, but complicated and unreliable. A series of field tests on driven steel pipe piles in Dunkirk, France have convinced that the shaft capacity in sand increased to several times the "static and fresh" capacity over years (Jardine et al. 2005, 2006). The strong aging effect is possibly attributed to the relaxation of soil arching at the circumferential direction with time.

Interface Shear in Calcareous Sand

Calcareous sand differs from siliceous sand because of its crushability and high compressibility. There is a lack of measurement of PLR for calcareous sand; thus, the plugging behavior in such sand, is unclear. A pipe pile in silica sand is likely to be more plugged than an identical pile in calcareous sand because greater friction may be formed inside the pipe. Friction fatigue also takes place in calcareous sand and the reduction rate is much greater than that in silica sand. An investigation into the shear zone reveals that more broken particles lead to thicker shear zone in calcareous sand (DeJong et al. 2003). Jardine et al. (2005) suggested that calcareous sand be treated as a nondilating and low-density sand. Hence, the increase in lateral effective stress, $\Delta\sigma'_r$, equals zero, and

the interface friction angle approaches a lower critical state value. Although the PLR employed in this study is capable of reflecting the difference in sand type, further improvement needs to include factors that account for the crushability.

Concluding Remarks

This study discusses the characteristics of the interface shear that is crucial for determining the radial effective stress on the pile shaft during installation and static loading. An effort has been made to develop a modified framework to correlate the soil-squeezing effect to the degree of soil plugging. The main conclusions are as follows:

1. The narrow shear zone adjacent to the pile shaft is responsible for the reduction in lateral effective stress and friction fatigue. The cyclic loading performance during installation is linked to the parameter of cycle number, which is associated with the contraction of shear zone and accumulation of shear slip displacement. They are also essential indicators for representing the behavior of friction decay of a working pile subjected to wind or wave. But for practical use, the more apparent depth index is instead preferred to reflect friction fatigue in several empirical design procedures.
2. The degree of soil plugging imposes an important effect on the shaft capacity by controlling the radial soil displacement during penetration. By introducing the soil-squeezing ratio, the stationary radial effective stress is correlated to the PLR in an inversely proportional manner, whereas the increase in radial effective stress afterward is positive with increasing PLR. The use of PLR in the modified approach also partly represents the influence of installation method on the shaft friction.
3. Case studies on offshore bridge piles in granular soils witness the importance of incorporating the features of small radial soil displacement and full decay in shaft friction into the capacity design. Comparison with the in situ measurement of the shaft capacity of two test piles reveals that the modification conducted in this study is capable of promoting the prediction accuracy.

Acknowledgments

The authors greatly appreciate all three reviewers for their detailed and constructive comments. This work is sponsored by the National Natural Science Foundation of China (41102179) and a grant from the University of Hong Kong (10208227).

References

Chin, J. T., and Poulos, H. G. (1996). "Tests on model jacked piles in calcareous sand." *Geotech. Test. J.*, 19(2), 164–180.

DeJong, J. T., Randolph, M. F., and White, D. J. (2003). "Interface load transfer degradation during cyclic loading: A microscale investigation." *Soils Found.*, 43(4), 81–93.

de Nicola, A., and Randolph, M. F. (1997). "The plugging behaviour of driven and jacked piles in sand." *Géotechnique*, 47(4), 841–856.

Fakharian, K., and Evgin, E. (1997). "Cyclic simple-shear behavior of sand-steel interfaces under constant normal stiffness condition." *J. Geotech. Geoenviron. Eng.*, 123(12), 1096–1105.

Geotechnical Engineering Office (. (2006). *Foundation design and construction*, Publication No. 1/2006, The Geotechnical Engineering Office of HKSARG, Hong Kong.

Jardine, R., Chow, F., Overy, R., and Standing, J. (2005). *ICP design methods for driven piles in sands and clays*, Thomas Telford, London.

Jardine, R. J., Standing, J. R., and Chow, F. C. (2006). "Some observations of the effects of time on the capacity of piles driven in sand." *Géotechnique*, 56(4), 227–244.

Kikuchi, Y., Mizutani, M., and Yamashita, H. (2007). "Vertical bearing capacity of large diameter steel pipe piles." *Proc. of Advances in Deep Foundations*, Taylor & Francis, London,177–182.

Lehane, B. M., Jardine, R. J., Bond, A. J., and Frank, R. (1993). "Mechanisms of shaft friction in sand from instrumented pile tests." *J. Geotech. Engrg. Div.*, 119(1), 19–35.

Lehane, B. M., Schneider, J. A., and Xu, X. (2005). *A review of design methods for offshore driven piles in siliceous sand*, Univ. of Western Australia, Perth, Australia.

Paik, K., and Salgado, R. (2004). "Effect of pile installation method on pipe pile behavior in sand." *Geotech. Test. J.*, 27(1), 1–11.

Paik, K., Salgado, R., Lee, J., and Kim, B. (2003). "Behavior of open- and closed-ended piles driven into sands." *J. Geotech. Geoenviron. Eng.*, 129(4), 296–306.

Poulos, H. G. (1989). "Cyclic axial loading analysis of piles in sand." *J. Geotech. Engrg. Div.*, 115(6), 836–852.

Randolph, M. F. (2003). "Science and empiricism in pile foundation design." *Géotechnique*, 53(10), 847–875.

Randolph, M. F., Dolwin, J., and Beck, R. (1994). "Design of driven piles in sand." *Géotechnique*, 44(3), 427–448.

Schneider, J. A., Xu, X., and Lehane, B. M. (2008). "Database assessment of CPT-based design methods for axial capacity of driven piles in siliceous sands." *J. Geotech. Geoenviron. Eng.*, 134(9), 1227–1244.

Uesugi, M., and Kishida, H. (1986). "Influential factors of friction between steel and dry sands." *Soils Found.*, 26(2), 33–46.

Uesugi, M., Kishida, H., and Tsubakihara, Y. (1989). "Friction between sand and steel under repeated loading." *Soils Found.*, 29(3), 127–137.

Wang, Y. (2008). *Review on the construction aspects of the Cross-Sea Bridge of Hangzhou Bay*, China Communications Press, Beijing (in Chinese).

White, D. J., and Bolton, M. D. (2002). *Observing friction fatigue on a jacked pile*. Centrifuge and constitutive modelling: Two extremes, Balkema, Rotterdam, Netherlands.

White, D. J., and Lehane, B. M. (2004). "Friction fatigue on displacement piles in sand." *Géotechnique*, 54(10), 645–658.

Xu, X., Schneider, J. A., and Lehane, B. M. (2008). "Cone penetration test (CPT) methods for end-bearing assessment of open- and closed-ended driven piles in siliceous sand." *Can. Geotech. J.*, 45(8), 1130–1141.

Yu, F., and Zhang, Z. M. (2011). "A design framework for evaluating the vertical bearing capacity of open-ended concrete pipe pile from empirical correlations." *China Civ. Eng. J.*, 44(7), 100–110 (in Chinese).